Since January 2020 Elsevier has created a COVID-19 resource centre with free information in English and Mandarin on the novel coronavirus COVID-19. The COVID-19 resource centre is hosted on Elsevier Connect, the company's public news and information website.

Science of the Total Environment 741 (2020) 140214

Contents lists available at ScienceDirect

Science of the Total Environment

journal homepage: www.elsevier.com/locate/scitotenv

Long-range air pollution transport in East Asia during the first week of the COVID-19 lockdown in China

Stephen Miles Griffith [a,*], Wei-Syun Huang [a], Chia-Ching Lin [b], Ying-Chieh Chen [b], Kuo-En Chang [c], Tang-Huang Lin [c], Sheng-Hsiang Wang [a], Neng-Huei Lin [a,b,**]

[a] Department of Atmospheric Sciences, National Central University, Taoyuan 32001, Taiwan
[b] Center for Environmental Monitoring and Technology, National Central University, Taoyuan 32001, Taiwan
[c] Center for Space and Remote Sensing Research, National Central University, Taoyuan 32001, Taiwan

HIGHLIGHTS

- COVID-19 lockdown in China reduced long-range transport of air pollution to Taiwan.
- OMI NO2 over central-north China reduced by 24% compared to previous years.
- PM2.5 concentration in northern Taiwan 2 times lower compared to similar episode
- CMAQ simulation with 50% reduced emission in China matches measured PM2.5 in Taiwan.
- Avoided PM2.5 pollution equivalent to 0.5 μg m^{-3} reduction for entire winter season

GRAPHICAL ABSTRACT

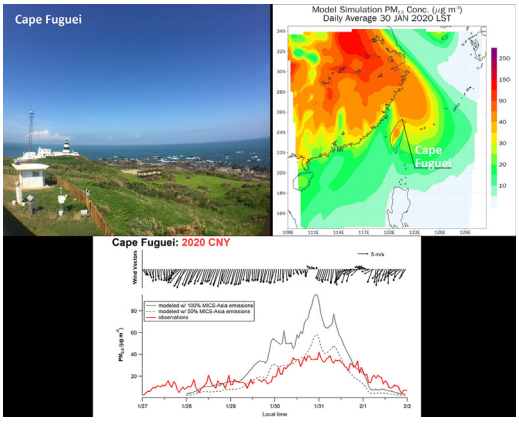

ARTICLE INFO

Article history:
Received 13 May 2020
Received in revised form 12 June 2020
Accepted 12 June 2020
Available online 15 June 2020

Keywords:
Transboundary aerosol
Taiwan
Shutdown
Emissions reduction
CMAQ
$PM_{2.5}$

ABSTRACT

Long-range transport (LRT) of air pollutants from East Asia during the northeast monsoon season impacts several downwind locations. In 2020, the initial COVID-19 lockdowns in China overlapped with Week 3 of the Chinese New Year (CNY) holiday, and an Asian outflow event. Thus, movement of the Chinese populace from city to city was already greatly reduced by the time of the LRT episode, although the reductions in industrial output are less clear. We found NO_2 column concentrations were reduced by 24% during the CNY Week 3 this year compared to previous years. The attenuated transport event arrived to northern Taiwan with a $PM_{2.5}$ concentration <45 μg m^{-3} and most often <35 μg m^{-3}, which is 2–3 times lower than LRT episodes of similar back-trajectory and synoptic patterns. The whole episode persisted for about 60 h, longer than most LRT episodes from China to Taiwan. CMAQ v5.2.1 modeling of the LRT event with 100% emission and reduced emission scenarios, revealed emissions in China were approximately 50% less than normal periods. Due to the length of the episode and the significant reduction in emissions, Taiwan avoided a $PM_{2.5}$ surplus of 19.2 μg m^{-3} on average during the episode, equivalent to a 0.5 μg m^{-3} reduction for the whole 3-month winter season. Employing the 100% emission model scenario and scaling up to the average episode hours each winter, the $PM_{2.5}$ surplus delivered via plumes on the northeast monsoon is equivalent to a 0.5 μg m^{-3} surplus for the whole year.

* Corresponding author.
** Correspondence to: N.-H. Lin, Department of Atmospheric Sciences, National Central University, 300 Zhongda Road, Taoyuan 32001, Taiwan.
E-mail addresses: stegriff88@gmail.com (S.M. Griffith), nhlin@cc.ncu.edu.tw (N.-H. Lin).

https://doi.org/10.1016/j.scitotenv.2020.140214
0048-9697/

1. Introduction

Transboundary aerosol (i.e. suspended liquid or solid particle in air) pollution impacts areas all around the world (Querol et al., 2004; Itahashi et al., 2017; Anil et al., 2019; Shairsingh et al., 2019; Grenier et al., 2020), and East Asia is a particularly unique arena for these events. From late autumn to early spring, northeast monsoon weather patterns are routine over East Asia and deliver air masses across the Asian continent (Luo et al., 2018), and as outflow from the continent across the East China Sea and to Korea (Lee et al., 2015; Kim et al., 2018), Japan (Matsuda et al., 2010; Kaneyasu et al., 2014; Lee et al., 2019) and Taiwan (Chuang et al., 2008; S.H. Wang et al., 2016; Hung et al., 2019; Kishcha et al., 2018). $PM_{2.5}$ (i.e. aerosols less than or equal to 2.5 μm in diameter) are a common component of these air masses as they are a conglomeration of hundreds if not thousands of different compounds, of which the less reactive and less volatile components are capable of long transport (Ueda et al., 2016; Shimada et al., 2018). Furthermore, $PM_{2.5}$ is a small-diameter subset of total particles, and thus is the most buoyant and can be easily carried on the wind. $PM_{2.5}$ transboundary events may be particularly intense if local pollution in the receptor area significantly mixes in with the transported plume (Hung et al., 2019). On the other hand, the incoming plume may completely dominate the total $PM_{2.5}$ concentration (Chuang et al., 2008; Kaneyasu et al., 2014). Some of these transboundary events in East Asia are dust-related, originate from one of two deserts in north-northwest China and are physically dominated by larger particles that completely occlude the visual range (Wang et al., 2010). Dust-related plumes are more common in late winter and springtime (Hung et al., 2019), while other transboundary plumes in East Asia are populated by anthropogenic sulfate particles and may arrive throughout the northeast monsoon season (Hung et al., 2019).

Taiwan is often a receptor for transboundary pollution coming from East Asia (Chuang et al., 2008; S.H. Wang et al., 2016; Chuang et al., 2017; Kishcha et al., 2018; Hsu and Cheng, 2019; Tseng et al., 2019). It is an island nation sitting just southeast of the main continental land mass of Asia and on the southern boundary of the East China Sea; thus during northeast monsoon season, it can be the recipient of even relatively small Asian outflow plumes. The mountainous terrain cutting through the center of Taiwan to the northeast disrupts the flow of low-altitude incoming air masses, essentially shielding eastern Taiwan from much of the brunt of the incoming wintertime plumes. On the other hand, western Taiwan is relatively more exposed, and combined with northern and southwest Taiwan, holds ~95% of Taiwan's population, leading to much greater exposure across the island. Distinguishing the impacts of local and transboundary pollution on public health in Taiwan is a frequent concern (Chan et al., 2008; Chien et al., 2012) that commonly brings scrutiny to the effectiveness of air pollution control policies.

In the midst of the wintertime, northeast monsoon season, Chinese New Year (CNY) is observed and changes the routine activities of populations in East Asia (Tan et al., 2013; Wang et al., 2017), while the industries continue at some partial capacity. CNY is a lunar calendar observance that can be characterized as a four-week period, although it spans different solar calendar dates each year. Holidays don't actually begin until the first day of the third week, Chinese New Year's Eve (i.e. the end of the lunar year) and continue on throughout the third week, although some of the population in China begins to travel back home even in the first week. By the middle of Week 3, the family gatherings have largely finished and the population moves again, this time towards vacationing or returning to their working city. However, COVID-19 emerged sometime in late 2019 and by Week 3 of CNY 2020, the disease was taking a heavy toll in Wuhan, the virus epicenter. Wuhan was locked down on Jan 23rd, the last day of CNY Week 2, followed by other municipal and provincial over the following few weeks. Thus, the population movement in China, post-holiday gatherings, was dramatically subdued during Week 3, but the industrial output is unclear. A multitude of workers, many of which hail from Hubei province, were stranded in their hometown; thus, industries were undoubtedly hobbled by not having their full workforce return, but the impact of this by late Week 3 is uncertain. From a model-measurement study, Li et al. (2020) determined that NO_x, VOCs and $PM_{2.5}$ emissions in the Yangtze River Delta (YRD) region were reduced by about 50% during the first month of the COVID-19 lockdown in China. On the other hand, Wang et al. (2020) simulated the COVID-19 lockdown emissions situation in China and found lesser emission reductions in the industrial and mobile sectors were needed to match $PM_{2.5}$ observations. They noted that high $PM_{2.5}$ episodes unfortunately were not avoided in the urban area due to unfavorable meteorology across the North China Plain. However, it is unclear how these buoyed $PM_{2.5}$ concentrations during the lockdown in China translated to transboundary pollution events.

Although a pandemic has not shut down wide swaths of Asia before, strategic city-wide pollution reduction actions have occurred in China, most notably during the Beijing 2008 Summer Olympics that temporarily shut down all construction activities in the city, reduced traffic by approximately half and increased the frequency of road cleanings by wet methods (Wang et al., 2009). These actions reduced columnar NO_2 densities by >40% and generally lowered ozone concentrations by up to 10 ppb even up to 100 km downwind (Wang et al., 2009; Witte et al., 2009). Asia-Pacific Economic Cooperation (APEC) conference in late 2014 again resulted in vast measures to improve the local air quality in Beijing and surrounding provinces (Huang et al., 2015; Y. Wang et al., 2016), including those implemented during the 2008 Olympics and a partial local industry shutdown; these measures successfully resulted in temporary NO_2 (vertical column densities) and atmospheric optical depth (AOD) improvements of ~50% and ~33%, respectively over the region. Furthermore, Shanghai and Zhejiang province were placed under strict pollution control measures for the G20 Summit in 2016 held in Hangzhou, Zhejiang that resulted in clear skies in the host city and $PM_{2.5}$ reductions of up to 50% in the megacity (Li et al., 2019). However, these dramatic emission perturbations were primarily local or partly regional, and studies of the impacts did not examine long-range transport out of the main Asian continental landmass. The COVID-19 pandemic, although ultimately devastating for humanity, has setup a unique situation, with very little precedent, to evaluate transboundary pollution intensity in the midst of a partial industry shutdown and population lockdown from a major source area, which also allows the receptor locations (e.g. Taiwan) to examine the transboundary contribution. This study examines such a case, where within days of the COVID-19 lockdown in Wuhan, a transboundary pollution plume was carried from Central-North China down to Taiwan by the northeast monsoon. This study uses ground-based measurements in Taiwan, satellite measurements covering East Asia, and chemical-transport simulations to evaluate the immediate impact of COVID-19 on a common transboundary pollution pathway.

2. Methods

2.1. Surface measurements

Hourly $PM_{2.5}$ concentrations from across Taiwan and hourly PM_{10} concentrations, CO mixing ratios, and wind speed and direction at Cape Fuguei were obtained from the Taiwan Air Quality Monitoring Network (https://airtw.epa.gov.tw). Cape Fuguei is located at the northern tip of Taiwan and juts out into the East China Sea, thus during northeast monsoon winds, local influence is negligible and the Cape Fuguei station acts as a bellwether for incoming long-range pollution (Chou et al., 2008; Lin et al., 2012; Pani et al., 2017).

2.2. HYSPLIT

Hybrid Single-Particle Lagrangian Integrated Trajectory (HYSPLIT v.4.9, NOAA Air Resources Laboratory) model (Draxler, 2003) was used to model 5-day back-trajectories from Cape Fuguei (25.29° N, 121.53° E). Meteorological input data for the back-trajectory calculation was the NCEP Global Data Assimilation System (GDAS) at 1° resolution.

2.3. OMI NO_2

Remotely sensed NO_2 from the OMI UV/Vis spectrometer aboard the NASA Aura satellite (Krotkov et al., 2016) was used to monitor emission activity over China. Slant column NO_2 densities are calculated from backscatter radiance measurements in the 405–465 nm spectral window of the spectrometer. OMI measures across a 2600 km swath at a minimum pixel size of 13 × 24 km^2, once a day at approximately 13:45 local time. The level-3 OMNO2d data product Total Tropospheric Column NO_2 for all atmospheric conditions was extracted for use. For this work, we averaged seven days together for comparing different weeks of the Chinese New Year.

2.4. CMAQ modeling

Community Multiscale Air Quality (CMAQ) v5.2.1 model was used to simulate a 2020 Chinese New Year transport episode. Simulations over East Asia used a nested domain structure with Taiwan at the center: from domain 1 (coarse, 81 km^2 pixel resolution) covering East Asia to progressively finer resolutions of 27 km^2, 9 km^2, and finally 3 km^2 at domain 4, which only included Taiwan. The meteorological component was simulated by Weather Research Forecast (WRF) model v3.9.1, where NCEP Final Operational Global Analysis 1° × 1° data (https://rda.ucar.edu/datasets/ds083.2/) were used as the initial condition. Anthropogenic emissions for Domains 1–3 were fed by Model Intercomparison Study for Asia (MICS-Asia) Phase III emission inventory (Li et al., 2017), while Domain 4 was fed by Taiwan Emission Database System 10 (TEDS, TWEPA, 2019, https://teds.epa.gov.tw/), with 2016 as the base year. Our work modified the MICS-Asia emissions of SO_2 (−62%), NO_x (−17%), NMVOC (+11%), NH_3 (+1%), CO (−27%), PM_{10} (−38%), $PM_{2.5}$ (−35%), BC (−27%), OC (−35%) and CO_2 (+18%) based on the relative changes of China's anthropogenic emissions between 2010 and 2017 (Zheng et al., 2018). Biogenic emissions were dictated by Biogenic Emission Inventory System version 3.09 (BEIS3, Vukovich and Pierce, 2002) for Taiwan and by Model of Emissions of Gases and Aerosols from Nature v2.1 (MEGAN, Guenther et al., 2012) for regions outside Taiwan.

3. Results

3.1. Satellite measurements

Fig. 1 shows the OMI total tropospheric column NO_2 concentrations averaged for each week of the Chinese New Year from 2017 to 2020. NO_2 is used as a proxy for general emission activity as it is too short-lived to make a significant impact in a transboundary episode from China to Taiwan, but is more readily detected without cloud interference by remote sensing than AOD from, for instance, the VIIRS satellite.

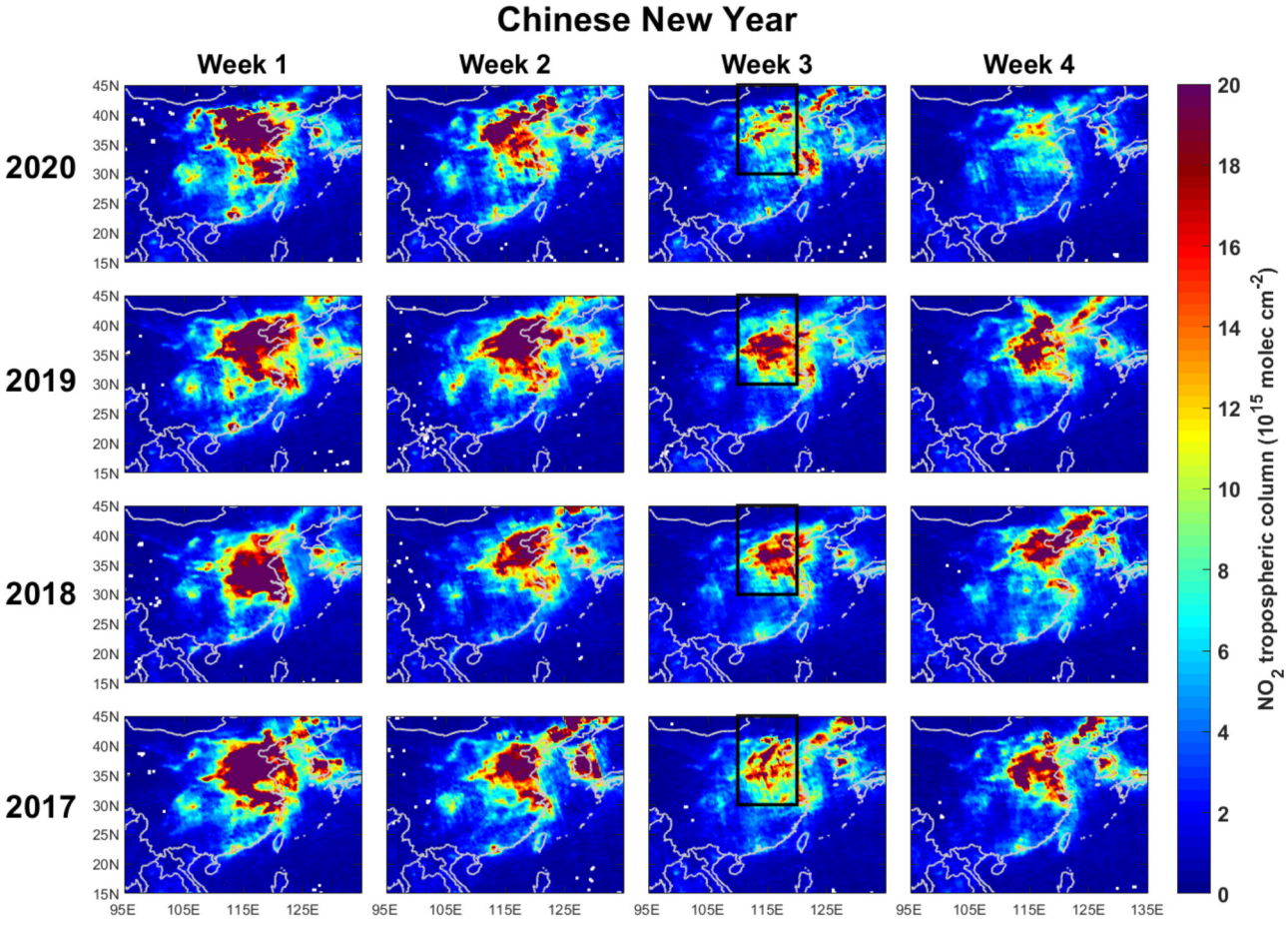

Fig. 1. OMI NO_2 weekly averages during Chinese New Year holiday periods from 2017 to 2020. The boxes in Week 3 outline the area from 30–45° N and 110–120° E.

As mentioned, some Chinese workers begin traveling even in Week 1, but Week 2 is a time of substantially more movement, particularly by the end of the week as New Year's Eve holiday nears. The beginning of Week 3 is the closest China comes to an annual stoppage of their population, thus Weeks 1 and 2 notably have greater NO_2 concentrations each year compared to Week 3, whereas Week 4 typically sees an increase in NO_2, although not back up to the Week 1 levels. Focusing on the area outlined by 30–45° N and 110–120° E, the NO_2 concentrations averaged 14.9×10^{15} molecules cm^{-2} and 11.0×10^{15} molecules cm^{-2} in Weeks 1 and 2 from 2017 to 2020, and averaged 8.3×10^{15} molecules cm^{-2} and 9.7×10^{15} molecules cm^{-2} in Weeks 3 and 4 from 2017 to 2019. In contrast, Weeks 3 and 4 in 2020 averaged only 6.4×10^{15} and 5.1×10^{15} NO_2 molecules cm^{-2}, representing 24% and 48% reductions, respectively, compared to the previous three years. In CNY Weeks 4–7 (i.e. Feb 2020), Xu et al. (2020) reported surface NO_2 concentrations had decreased by 61.4% compared to the same time in 2017–2019, which was three times steeper than the Week 3 decrease noted here, likely due to the broader lockdown across the whole of China.

Wuhan and other cities in Hubei province were put on lockdown starting from Jan 23rd, the last day of what is considered CNY Week 2 in this work, while lockdowns outside Hubei began from Feb 2nd onward. However, the shutdown timeline of industries in China during the COVID-19 outbreak is less clear, and was likely spatially and temporally variable.

3.2. Surface charts and trajectories

This work examines a long-range transport episode of a pollution plume from China that arrived in Taiwan towards the end of CNY Week 3 and would have been fueled by China emissions in the middle of CNY Week 3. Fig. 2a displays the surface chart from Jan 29th 1800 UTC (Jan 30th 0200 LT), which was approximately the arrival time of the long-range transport event. A surface high pressure system had migrated down to Southeast Asia and was bringing northerly to northeasterly winds to Taiwan. The 1020 hPa isobar traces back from Taiwan along the eastern coast of China and over the northeastern provinces of China, a typical surface pattern for a northeasterly monsoon event in Taiwan. Back-trajectories clearly show transport to Taiwan from North China over the preceding days (Fig. 2b). All of the trajectories passed through or originated in the latitude – longitude coordinate boundaries (i.e. black outline) detailed in the OMI NO_2 data presentation.

3.3. Surface $PM_{2.5}$ measurements

Fig. 3 shows the arrival and southward transport of the pollution plume through Taiwan. In the early hours of Jan 30th, 2020, the $PM_{2.5}$ concentration at the coast of northern Taiwan (e.g. Cape Fuguei) began to increase from around 10 μg m^{-3} to >25 μg m^{-3}, representing

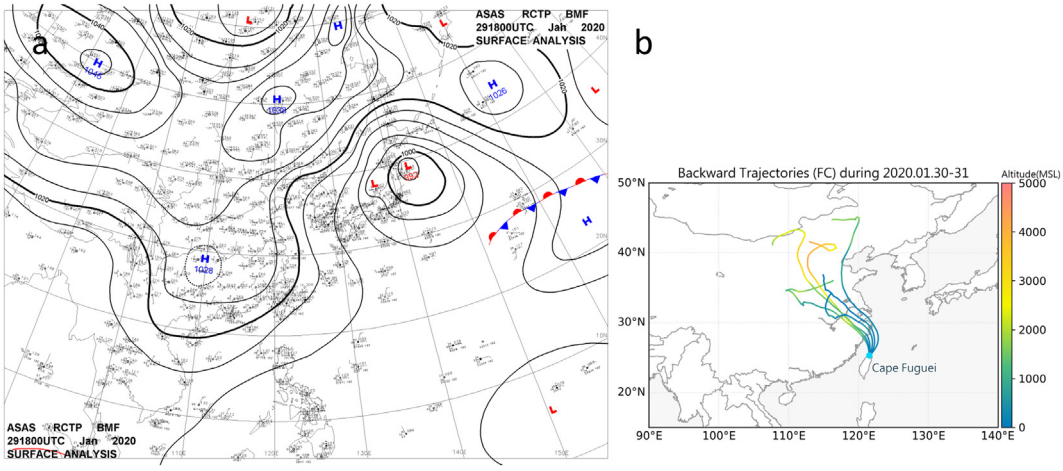

Fig. 2. a) Surface chart at the onset of the long-range transport event, and b) 5-day back-trajectories arriving at a 100 m height every 8 h from 0300 LT on Jan 30th to 1900 LT on Jan 31st, 2020.

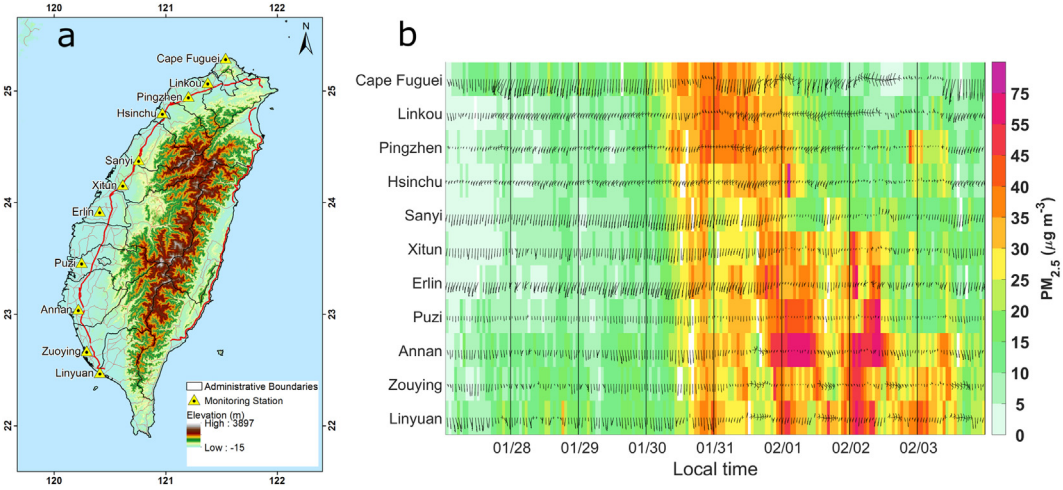

Fig. 3. Latitudinal $PM_{2.5}$ concentrations and wind speed/direction in Taiwan during a 2020 CNY long-range transport event (Linkou is a district of New Taipei City; Pingzhen a district of Taoyuan; Sanyi a district in Miaoli; Xitun a district of Taichung; Erlin a district of Changhua; Puzi a district of Chiayi; Annan a district of Tainan; and Zuoying and Linyuan are districts of Kaosiung).

the onset of the event. Over the course of Jan 30th, the leading edge of the plume migrated south reaching the Kaosiung area (i.e. Zuoying and Linyuan) around noontime. The $PM_{2.5}$ concentrations at Cape Fuguei progressively increased and briefly topped 40 μg m^{-3} in the first half of Jan 31st. Meanwhile, the southward moving plume encountered slower wind speeds and local pollution (e.g. Linkou and Pingzhen) further inland in northern Taiwan, allowing the $PM_{2.5}$ concentration to remain more frequently above 40 μg m^{-3}. Then the flow of the plume was likely interrupted by the western edge of the Xueshan mountain range causing multidirectional flow from that point. Pushing on through western Taiwan (e.g. Xitun) at higher wind speeds, the average $PM_{2.5}$ concentrations peaked at a lower concentration than in northern Taiwan. By the time of reaching southern Taiwan, the plume had likely disbanded into multiple streams and $PM_{2.5}$ concentrations only sporadically increased above 35 μg m^{-3} further southward (e.g. Zuoying) until the end of Jan 31st. Eventually, the plume began to weaken in concentration and by early morning 01 Feb, 2020, $PM_{2.5}$ concentrations dropped below 25 μg m^{-3} in northern Taiwan. However, the waning plume again encountered lower wind speeds and local pollution, this time in western and southwestern Taiwan (e.g. Annan), allowing accumulation above 45 μg m^{-3} in many areas and even above 75 μg m^{-3} in the most severe locations.

For comparison, Fig. 4 shows another long-range transport event that occurred on Feb 1st, 2018, and in many respects was similar to the 2020 CNY event detailed above. Firstly, a high-pressure system was bearing down on Southeast Asia and Taiwan, and the trajectories hailed from the same broad swath as the aforementioned event (Fig. S1). Second, high $PM_{2.5}$ concentrations transported from north to south Taiwan and were exacerbated by low wind speeds in parts of Taiwan and alleviated by higher wind speeds in other parts. A final important similar characteristic for both episodes is the absence of a strong dust component at the surface level. Fig. S4 shows Lidar returns (NRB and volume depolarization ratio) for both events, from a site in northern Taiwan that is ~50 km southwest of Cape Fuguei, revealing that dust resided at 2 km and 5 km altitude, but not at the surface during the CNY 2020 episode. Furthermore, the $PM_{2.5}/PM_{10}$ ratio (not shown here) indicates the dust particles were not dominant during these two episodes. On the other hand, the differences between these two events are distinct. The amount of total tropospheric column NO_2 measured over China was much higher during the Feb. 2018 event (Fig. S2) by a factor of ~2.5, and the AOD over the source area as measured from the VIIRS satellite was clearly more widespread during the 2018 event (Fig. S3), although cloud cover severely reduced the useable data in both years. Likely as a result of the source area differences, the peak $PM_{2.5}$ concentrations on arrival to Taiwan were higher than 71 μg m^{-3}, a factor of 2 or more than the 2020 CNY episode. To note, approximately 30 mm of rain fell in northern Taiwan (not shown here) during the Feb 2018 episode, likely attenuating the PM2.5 concentrations that were on the verge of transporting throughout Taiwan, causing these two episodes to be closer in concentration than otherwise. Another characteristic difference of these two events is the 02/2018 plume was associated with strong northeasterly winds upon arrival, whereas lighter northerly winds were characteristic of the 2020 CNY episode. The arrival wind speeds may have impacted the overall length of the episodes as the 02/2018 episode was only ~24 h, and the incoming $PM_{2.5}$ concentrations dramatically reduced by nearly a factor of 3 in only a few hours, while the CNY 2020 episode persisted for ~60 h. These episode durations bracket the average transboundary Chinese haze episode length, 35 h, reported by S.H. Wang et al. (2016) for northern Taiwan from 2005 to 2014. Overall, LRT transport plumes arriving from East Asia peak in concentration between ~45 μg m^{-3} (Chuang et al., 2017; Hung et al., 2019) to >100 μg m^{-3} (S.H. Wang et al., 2016), where most of the variability is introduced from factors such as meteorology, trajectory path and dust influence.

3.4. CMAQ simulations

In an effort to simulate the CNY 2020 plume arriving from the source area to Taiwan, CMAQ v5.2.1 with two different emission scenarios was used to model the period of Jan 30th–Feb 1st, 2020. As mentioned in the Methods section, the MICS-Asia emission inventory (i.e. East Asia) was modified based on the relative changes of China's anthropogenic emissions between 2010 and 2017 (Zheng et al., 2018). In our two scenarios, we then used 100% and 50% of the modified MICS-Asia emissions in an attempt to simulate 'situation normal' and 'lockdown of the public and partial shutdown of industry in China' scenarios. Fig. 5 shows the simulation results from Jan 30th–Feb 1st for $PM_{2.5}$ concentrations within the 81 km resolution domain 3 under the 100% emissions scenario. Already by the early hours (0000 LT) of Jan 30th, the Asian outflow plume was jutting out southeast of the Shanghai area and abut with northeast Taiwan. Simulated $PM_{2.5}$ concentrations in northern Taiwan had reached above 50 μg m^{-3} by this point, more than a factor of 2 greater than the observations in Fig. 3. The outflow plume then swung southwest while spreading further outward, resulting in peak $PM_{2.5}$ concentrations of approximately 100 μg m^{-3} in northern Taiwan around 0000 LT on Jan 31st, nearly a factor of 3 greater than the observations.

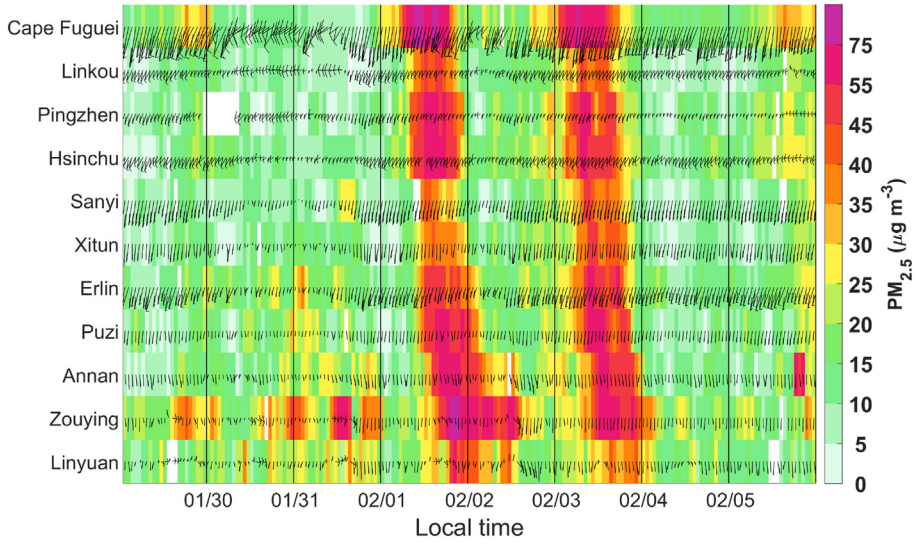

Fig. 4. Latitudinal $PM_{2.5}$ concentrations and wind speed/direction in Taiwan during a 02/2018 long-range transport event. This study uses the 02/01 episode for comparison. The 02/03 event was more influenced by dust.

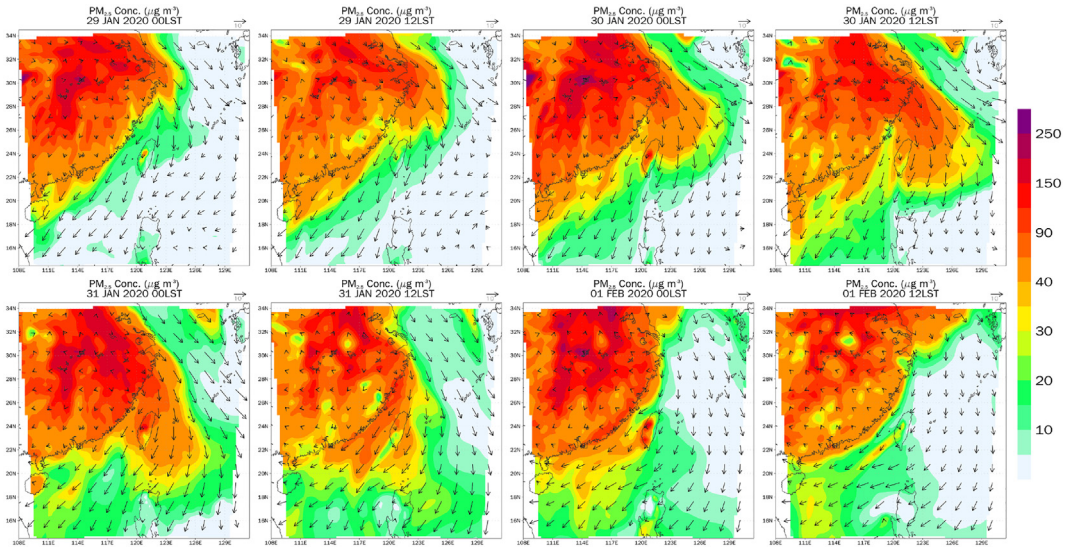

Fig. 5. CMAQ v5.2 modeling simulations of the CNY 2020 event using 100% MICS-Asia emissions.

The plume kept swinging to the west-southwest, eventually leaving Taiwan with remnants of the plume accumulated with local pollutants in west and southwest Taiwan around 0000 LT on Feb 1st, which was also observed in Fig. 3 above.

On the other hand, Fig. 6 shows the simulation results from the 50% MICS-Asia emissions scenario where the Asian outflow plume is still jutting out southeast of the Shanghai area, but $PM_{2.5}$ concentrations ~50 μg m^{-3} are only barely extended out into the East China Sea rather on the doorstep of northern Taiwan. Moreover, plume concentrations ~100 μg m^{-3} are never transported off the coast of China in this scenario, and the peak in northern Taiwan, as might be expected, is approximately half of that in the 100% emissions scenario. Furthermore, the remnant concentrations in west-southwest Taiwan from the plume accumulation with local pollution at 0000 LT on Feb 1st was noticeably less severe in concentration and breadth in this reduced emissions scenario. To note, the local TEDS inventory was not reduced in this 50% scenario, thus the reduced $PM_{2.5}$ concentrations observed here were mostly due to reduced MICS-Asia emissions.

Fig. 7 shows the time series comparing the $PM_{2.5}$ observations at Cape Fuguei to the modeling results from the two scenarios. Clearly, in terms of intensity of the $PM_{2.5}$ peak, the 50% emissions scenario more closely matched the observations. In fact, the 100% emission scenario simulated two waves of $PM_{2.5}$ arriving around 0000 LT on Jan 30th and 0000 LT Jan 31st, while the 50% emissions scenario simulated severely attenuated versions of these peaks where the earlier peak was barely visible outside of the general rise in $PM_{2.5}$ concentration at that time. Although the first simulated $PM_{2.5}$ concentration peak (0000 LT, Jan 30th) did not register in the observation data, it did correspond to an increase in observation-based $PM_{2.5}/PM_{10}$ ratio and a decrease in CO, indicating a characteristic change in the pollution composition and signaled the onset of the episode. The $PM_{2.5}/PM_{10}$ ratio generally increased during the first 24 h of the episode, from around 0.2 to 0.5, indicating the plume was increasingly influenced by fine particles. At the time of the true episode peak in $PM_{2.5}$ concentration (~0000 LT Jan 31st), the $PM_{2.5}/PM_{10}$ ratio increased abruptly to ~0.7 and coincided with a drop in wind speed and increased modeled $PM_{2.5}$ concentrations, but not a sharp increase in observed $PM_{2.5}$. Thus, the plume migration into Taiwan largely stopped at this time and with it much of the coarse-mode aerosols within, leaving the already transported fine particles to dominate while the remaining coarse particles likely were

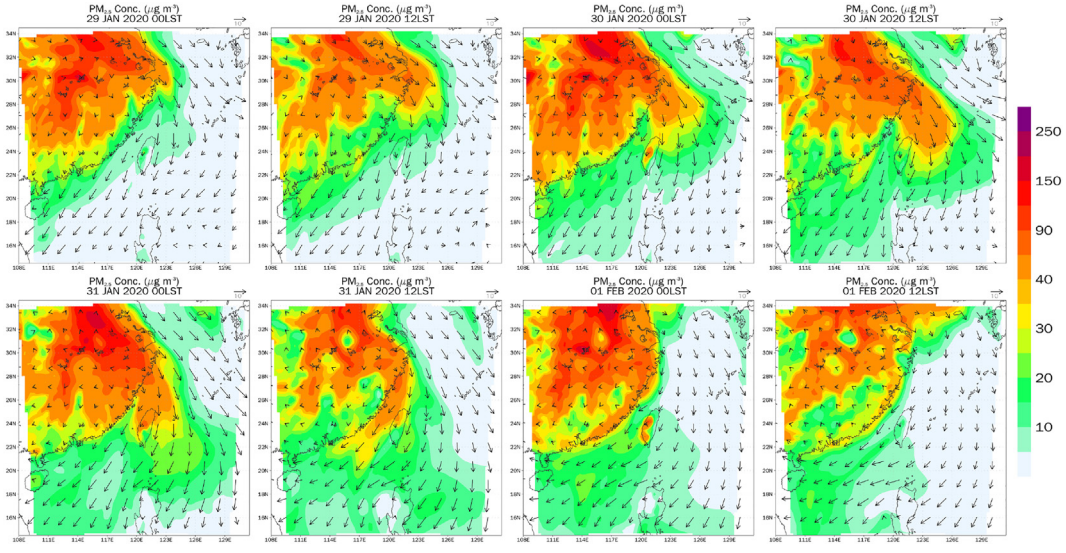

Fig. 6. CMAQ v5.2 modeling simulations of the CNY 2020 event using 50% MICS-Asia emissions.

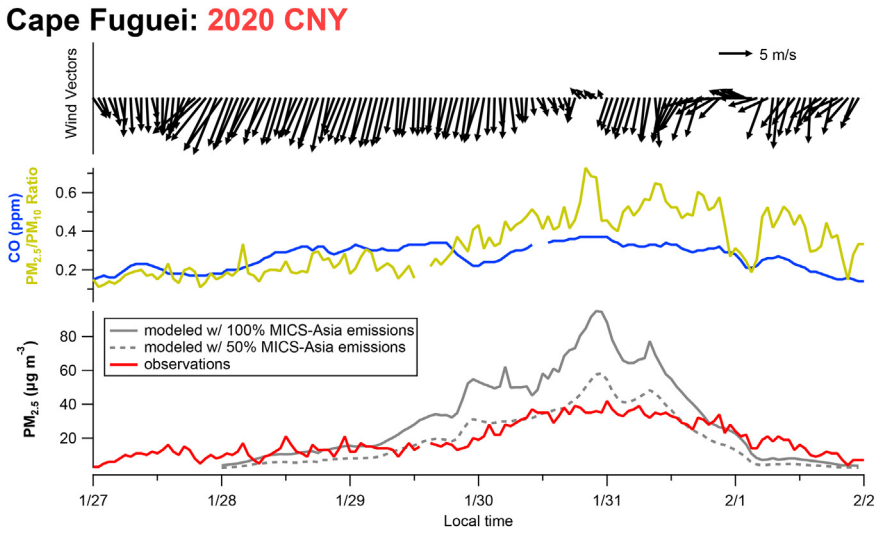

Fig. 7. Time series comparison of measured and modeled $PM_{2.5}$ mass concentrations at Cape Fuguei measurement station.

diminished from loss due to deposition. Starting from the evening of Jan 31st, the observed $PM_{2.5}$ concentration and the $PM_{2.5}/PM_{10}$ ratio began to decrease while the simulated $PM_{2.5}$ concentration decreased even more resulting in an underprediction of the observed values by the 50% emissions scenario. This discrepancy is likely due to modeled wind speeds (*not shown here*) at the tip of northern Taiwan that were lower than the measured values by ~2 m s^{-1} starting from around the evening of Jan 31st. This would result in less effective transport of the plume in the model whereas the plume was just weakening per the observations and not reducing in concentration so dramatically. Amidst the decrease in $PM_{2.5}$ concentrations, there was also a shift in wind direction to easterly flow over a period of ~6 h before returning to northerly flow, which was associated with a steep decrease in the $PM_{2.5}/PM_{10}$ ratio. Overall, the long-range transport episode at the end of CNY 2020 Week 3 was more accurately simulated by the MICS-Asia 50% emissions scenario, which aligns with a broad reduction in industrial emissions during that time.

Distinguishing the impacts of CNY and the COVID-19 shutdown on emissions reduction in China is complex. During CNY, the population is on the move before settling in for the holiday, thus inevitably leading to reduced traffic emissions during the first days of the third week. Wang et al. (2017) analyzed the impacts of the 2014 CNY in Shenzhen, which is in southern China, near Hong Kong, and found >50% of the residents departed the city, traffic on the roads was at 50% normal levels and NO_x, volatile organic compounds (VOCs), and primary organic aerosol concentrations decreased between 50 and 80%. However, Shenzhen is known to have the largest population of so-called floating workers in China, people that only reside in Shenzhen for work but travel back to elsewhere in China for holidays. Moreover, Shenzhen is not in the back-trajectory path of the CNY 2020 episode analyzed in this study, thus, the CNY conditions in Shenzhen cannot be assumed for the whole of central-northern China. Li et al. (2020) focused on the YRD region and implemented approximately 80% emission reductions for the traffic sector and 20–40% emission reductions for the industrial sector to match PM2.5 observations, which reduced by >20 μg m^{-3} compared to the pre-lockdown period, implying that the impact from the COVID-19 lockdown on reduced traffic emissions was at least an additional 30% over the CNY traffic reductions. On the other hand, in a broader survey across China, Wang et al. (2020) found 40% emission reductions for the traffic sector and 20% emission reductions for the industrial sector matched the $PM_{2.5}$ observations in some cities, including Shanghai, which decreased by <10 μg m^{-3} in a reduced emissions model. Wang et al. (2020) found that unfavorable meteorological conditions in China prevented a dramatic improvement in air quality there through Feb 12, 2020, three weeks after the Wuhan lockdown. This stands in contrast to the analysis of Xu et al. (2020) that examined the whole of Feb. 2020 and found significant reductions in a number of criteria pollutant concentrations, similar to past strategic shutdowns, such as APEC 2014. Nevertheless, an effective 50% reduction in East Asia emissions preceding arrival of the late Jan. 2020 plume to Taiwan, and corresponding in time to an overlap of CNY and the beginnings of the COVID-19 lockdowns in China, resulted in matching modeled and measured $PM_{2.5}$ concentrations in northern Taiwan.

4. Implications and conclusion

The city and provincial lockdowns in China stemming from the tragic COVID-19 outbreak afford the opportunity to examine the impact of emission changes from a major LRT source area to receptor areas in East Asia. Local and long-range transported air pollution impacts are often debated in Taiwan (Lin et al., 2007; Chuang et al., 2017; Kishcha et al., 2018), and this LRT episode during unexpected emission reductions is a further contribution. Through a meticulous accounting system developed by S.H. Wang et al. (2016) for identifying LRT haze episodes, Hung et al. (2019) determined that 2–8 LRT plumes impacted Taiwan every winter (Dec.–Feb.) from 2005 to 2015, occupying ~127 h of the season each year. Thus, the CNY 2020 episode (~60 h) examined in this study already accounted for nearly half of the LRT winter average duration in northern Taiwan. The reduced $PM_{2.5}$ concentration, peaking around 40 μg m^{-3} upon arrival to Taiwan, over the relatively long episode duration translated to a greatly reduced exposure. In normal times, a typical long-range transport episode coming from central-north China to Taiwan can bring $PM_{2.5}$ concentrations upwards of 70 μg m^{-3}, more than doubling the local concentration in some cases (e.g. Feb 2018 episode), and negatively impacting ~95% of the island's population, from northern Taiwan down the west coast to southern Taiwan. By using the median of the 72 h period (12 μg m^{-3}) preceding the increase in $PM_{2.5}$ concentration at Cape Fuguei, we can approximate the $PM_{2.5}$ surplus delivered by the plume as 17.3 μg m^{-3} on average during the 60 h episode. Moreover, under the 100% MICS-Asia emissions model, the $PM_{2.5}$ surplus was 36.5 μg m^{-3}. Thus, the $PM_{2.5}$ pollution avoided by this emissions reduction is equivalent to 0.5 μg m^{-3} each hour of the Dec-Feb winter season. Multiplying the model surplus calculation by 127 h, the average LRT episode hours delivered by the northeast monsoon as determined by Hung et al. (2019), is equivalent to a surplus of 2.1 μg m^{-3} each hour over the entire 3-month winter period, or 0.5 μg m^{-3} each hour over the

whole year. From a local perspective, these values can be viewed as targets for lowering local $PM_{2.5}$ contribution to counter the impact from LRT air pollution from continental East Asia. Taiwan has been addressing local pollution with steps to phase in electric vehicles, including motorcycles, private cars, and buses, and to subsidize the replacement of aging heavy-duty vehicles, which are projected to gradually improve the overall air quality (Lin et al., 2020). As $PM_{2.5}$ mass concentration pollution is potentially doubled during LRT events and their effects broadly felt across the vast majority of Taiwan communities, temporary local PM emission reductions in anticipation of a LRT event may also be explored as a way to supplement the current long-term efforts and minimize the negative health impacts, particularly in areas of Taiwan that are prone to stagnant winds during the northeast monsoon. Stifling the accumulation that occurs during these LRT events could address these spikes in $PM_{2.5}$ pollution, which affect the health and livelihood (e.g. visibility) of the island's population, in the face of continued intense emissions from continental East Asia. However, these adjustments would be only temporary remedies to counter severe spikes in pollution, whereas chronic exposure from accumulation of local emissions should be persistently addressed through the policy measures noted above.

Although concentrations of toxic compounds were not measured for this study, we may speculate as to their reduced concentrations and the implications. Chi et al. (2014) found elevated concentrations (>70% above non-episode times) of polychlorinated dibenzo-p-dioxins and dibenzofurans (PCDD/Fs) in PM_{10} during a northeast monsoon-driven LRT episode in Dec 2008. Reduced emissions of PCDD/Fs by 50% could be reasonably assumed for the CNY 2020 LRT event, halving their risk to the environment. PCDD/Fs are eventually introduced to the environment through particle deposition where they may then interact with soil and aquatic ecosystems, bioaccumulate and be ingested by the public (Suryani et al., 2015). Moreover, PCDD/Fs are toxic to other organisms (Tumasonis et al., 1973; Gilbertson, 1983; Gray et al., 1997), and thus high-altitude, fragile environments like at Mt. Lulin (Wai et al., 2008; Nguyen and Sheu, 2019) in central Taiwan may be relatively more protected by a reduction in East Asia emissions.

This examined episode in this study is a valuable window into how reduced emissions from China could impact $PM_{2.5}$ concentrations in Taiwan, decreasing the concentrations by approximately 50% in this case. However, a blanket 50% emission reduction scenario in China is likely not spatially representative of what really occurred during the exceptional time of the virus outbreak. Rather, the 50% reductions in the model act as a general test for massively reduced source emissions and the associated outcome at the receptor site. Industry shutdowns across China at this time were likely not only more spatially heterogeneous than simulated in this study, but also more temporally variable, with some lag in the shutdown from one region to another. Thus, to more precisely track the pollution reduction impacts due to COVID-19, further analysis efforts should be undertaken to more elegantly modify the MICS-Asia emissions inventory for this and subsequent time periods during the COVID-19 pandemic. Furthermore, Asian outflow LRT episodes are capable of impacting multiple sites across the East China Sea all in one swoop. We are awaiting the reports from sites (e.g. from Japan and Korea) that experienced similar reduced $PM_{2.5}$ pollution impacts during the same period.

CRediT authorship contribution statement

Stephen Miles Griffith: Conceptualization, Methodology, Formal analysis, Investigation, Writing - original draft, Visualization, Supervision, Project administration. **Wei-Syun Huang:** Methodology, Software, Formal analysis, Data curation, Visualization. **Chia-Ching Lin:** Formal analysis, Visualization. **Ying-Chieh Chen:** Formal analysis, Visualization. **Kuo-En Chang:** Formal analysis, Visualization. **Tang-Huang Lin:** Conceptualization, Resources. **Sheng-Hsiang Wang:** Resources, Writing - review & editing. **Neng-Huei Lin:** Conceptualization, Methodology, Resources, Writing - review & editing, Supervision, Project administration, Funding acquisition.

Declaration of competing interest

The authors declare that they have no known competing financial interests or personal relationships that could have appeared to influence the work reported in this paper.

Acknowledgements

This work was supported by Ministry of Science and Technology research grants (no. 107-2111-M-008-337 and 108-2811-M-008-513), and the National Central University New Research Staff Grant. We thank Taiwan Environmental Protection Administration for funding and use of their monitoring station data (https://airtw.epa.gov.tw), and NASA for use of their satellite product data. In addition, we thank Prof. C.-T. Lee and Dr. Charles C.-K. Chou for contributing to the model verification.

Appendix A. Supplementary data

Supplementary data to this article can be found online at https://doi.org/10.1016/j.scitotenv.2020.140214.

References

Anil, I., Alagha, O., Blaisi, N.I., Mohamed, I.A., Barghouthi, M.H., Manzar, M.S., 2019. Source identification of episodic rain pollutants by a new approach: combining satellite observations and backward air mass trajectories. Aerosol Air Qual. Res. 19 (12), 2827–2843. https://doi.org/10.4209/aaqr.2019.04.0187.

Chan, C.C., Chuang, K.J., Chen, W.J., Chang, W.T., Lee, C. Te, Peng, C.M., 2008. Increasing cardiopulmonary emergency visits by long-range transported Asian dust storms in Taiwan. Environ. Res. 106 (3), 393–400. https://doi.org/10.1016/j.envres.2007.09.006.

Chi, K.H., Chou, C.C.K., Peng, C.M., Chang, M.B., Lin, C.Y., Li, C.T., 2014. Increase of ambient PCDD/F concentrations in northern Taiwan during Asian dust storm and winter monsoon episodes. Aerosol Air Qual. Res. 14 (4), 1279–1291. https://doi.org/10.4209/aaqr.2013.03.0097.

Chien, L.C., Yang, C.H., Yu, H.L., 2012. Estimated effects of Asian dust storms on spatiotemporal distributions of clinic visits for respiratory diseases in Taipei children (Taiwan). Environ. Health Perspect. 120 (8), 1215–1220. https://doi.org/10.1289/ehp.1104417.

Chou, C.C.K., Lee, C.T., Yuan, C.S., Hsu, W.C., Lin, C.Y., Hsu, S.C., Liu, S.C., 2008. Implications of the chemical transformation of Asian outflow aerosols for the long-range transport of inorganic nitrogen species. Atmos. Environ. 42 (32), 7508–7519. https://doi.org/10.1016/j.atmosenv.2008.05.049.

Chuang, M.T., Fu, J.S., Jang, C.J., Chan, C.C., Ni, P.C., Lee, C. Te, 2008. Simulation of long-range transport aerosols from the Asian continent to Taiwan by a southward Asian high-pressure system. Sci. Total Environ. 406 (1–2), 168–179. https://doi.org/10.1016/j.scitotenv.2008.07.003.

Chuang, M.T., Chou, C.C.K., Lin, N.H., Takami, A., Hsiao, T.C., Lin, T.H., Fu, J.S., Pani, S.K., Lu, Y.R., Yang, T.Y., 2017. A simulation study on PM2.5 sources and meteorological characteristics at the northern tip of Taiwan in the early stage of the Asian haze period. Aerosol Air Qual. Res. 17 (12), 3166–3178. https://doi.org/10.4209/aaqr.2017.05.0185.

Draxler, R.R., 2003. Evaluation of an ensemble dispersion calculation. J. Appl. Meteorol. 42, 308–317.

Gilbertson, M., 1983. Etiology of chick edema disease in herring gulls in the lower Great Lakes. Chemosphere 12 (3), 357–370.

Gray, L.E., Ostby, J.S., Kelce, W.R., 1997. A dose-response analysis of the reproductive effects of a single gestational dose of 2,3,7,8-tetrachlorodibenzo-p-dioxin in male Long Evans hooded rat offspring. Toxicol. Appl. Pharmacol. 146 (1), 11–20. https://doi.org/10.1006/taap.1997.8223.

Grenier, P., Elliott, J.E., Drouillard, K.G., Guigueno, M.F., Muir, D., Shaw, D.P., Wayland, M., Elliott, K.H., 2020. Long-range transport of legacy organic pollutants affects alpine fish eaten by ospreys in western Canada. Sci. Total Environ. 712, 135889. https://doi.org/10.1016/j.scitotenv.2019.135889.

Guenther, A.B., Jiang, X., Heald, C.L., Sakulyanontvittaya, T., Duhl, T., Emmons, L.K., Wang, X., 2012. The model of emissions of gases and aerosols from nature version 2.1 (MEGAN2.1): an extended and updated framework for modeling biogenic emissions. Geosci. Model Dev. 5 (6), 1471–1492. https://doi.org/10.5194/gmd-5-1471-2012.

Hsu, C.H., Cheng, F.Y., 2019. Synoptic weather patterns and associated air pollution in Taiwan. Aerosol Air Qual. Res. 19 (5), 1139–1151. https://doi.org/10.4209/aaqr.2018.09.0348.

Huang, K., Zhang, X., Lin, Y., 2015. The "APEC Blue" phenomenon: regional emission control effects observed from space. Atmos. Res. 164–165, 65–75. https://doi.org/10.1016/j.atmosres.2015.04.018.

Hung, W.T., Lu, C.H. (Sarah), Wang, S.H., Chen, S.P., Tsai, F., Chou, C.C.K., 2019. Investigation of long-range transported PM2.5 events over Northern Taiwan during 2005–2015 winter seasons. Atmos. Environ. 217 (August), 116920. https://doi.org/10.1016/j.atmosenv.2019.116920.

Itahashi, S., Uno, I., Osada, K., Kamiguchi, Y., Yamamoto, S., Tamura, K., Wang, Z., Kurosaki, Y., Kanaya, Y., 2017. Nitrate transboundary heavy pollution over East Asia in winter. Atmos. Chem. Phys. 17 (6), 3823–3843. https://doi.org/10.5194/acp-17-3823-2017.

Kaneyasu, N., Yamamoto, S., Sato, K., Takami, A., Hayashi, M., Hara, K., Kawamoto, K., Okuda, T., Hatakeyama, S., 2014. Impact of long-range transport of aerosols on the PM2.5 composition at a major metropolitan area in the northern Kyushu area of Japan. Atmos. Environ. 97 (January 2013), 416–425. https://doi.org/10.1016/j.atmosenv.2014.01.029.

Kim, C.H., Lee, H.J., Kang, J.E., Jo, H.Y., Park, S.Y., Jo, Y.J., Lee, J.J., Yang, G.H., Park, T., Lee, T., 2018. Meteorological overview and signatures of long-range transport processes during the MAPS-Seoul 2015 campaign. Aerosol Air Qual. Res. 18 (9), 2173–2184. https://doi.org/10.4209/aaqr.2017.10.0398.

Kishcha, P., Wang, S.H., Lin, N.H., Silva, A. da, Lin, T.H., Lin, P.H., Liu, G.R., Starobinets, B., Alpert, P., 2018. Differentiating between local and remote pollution over Taiwan. Aerosol Air Qual. Res. 18 (7), 1788–1798. https://doi.org/10.4209/aaqr.2017.10.0378.

Lee, K., Kim, Y.J., Kang, C.H., Kim, J.S., Chang, L.S., Park, K., 2015. Chemical characteristics of long-range-transported fine particulate matter at Gosan, Jeju island, in the spring and fall of 2008, 2009, 2011, and 2012. J. Air Waste Manag. Assoc. 65 (4), 445–454. https://doi.org/10.1080/10962247.2014.1001883.

Krotkov, N.A., McLinden, C.A., Li, C., Lamsal, L.N., Celarier, E.A., Marchenko, S.V., Swartz, W.H., Bucsela, E.J., Joiner, J., Duncan, B.N., Boersma, K.F., Veefkind, J.P., Levelt, P.F., Fioletov, V.E., Dickerson, R.R., He, H., Lu, Z., Streets, D.G., 2016. Aura OMI observations of regional SO2 and NO2 pollution changes from 2005 to 2015. Atmos. Chem. Phys. 16, 4605–4629. https://doi.org/10.5194/acp-16-4605-2016.

Lee, K., Chandra, I., Seto, T., Inomata, Y., Hayashi, M., Takami, A., Yoshino, A., Otani, Y., 2019. Aerial observation of atmospheric nanoparticles on Fukue Island, Japan. Aerosol Air Qual. Res. 19 (5), 981–994. https://doi.org/10.4209/aaqr.2018.03.0077.

Li, M., Zhang, Q., Kurokawa, J.I., Woo, J.H., He, K., Lu, Z., Ohara, T., Song, Y., Streets, D.G., Carmichael, G.R., Cheng, Y., Hong, C., Huo, H., Jiang, X., Kang, S., Liu, F., Su, H., Zheng, B., 2017. MIX: a mosaic Asian anthropogenic emission inventory under the international collaboration framework of the MICS-Asia and HTAP. Atmos. Chem. Phys. 17 (2), 935–963. https://doi.org/10.5194/acp-17-935-2017.

Li, H., Wang, D., Cui, L., Gao, Y., Huo, J., Wang, X., Zhang, Z., Tan, Y., Huang, Y., Cao, J., Chow, J.C., Lee, S. cheng, Fu, Q., 2019. Characteristics of atmospheric PM2.5 composition during the implementation of stringent pollution control measures in shanghai for the 2016 G20 summit. Sci. Total Environ. 648, 1121–1129. https://doi.org/10.1016/j.scitotenv.2018.08.219.

Li, L., Li, Q., Huang, L., Wang, Q., Zhu, A., Xu, J., Liu, Z., Li, H., Shi, L., Li, R., Azari, M., Wang, Y., Zhang, X., Liu, Z., Zhu, Y., Zhang, K., Xue, S., Ooi, M.C.G., Zhang, D., Chan, A., 2020. Air quality changes during the COVID-19 lockdown over the Yangtze River Delta Region: an insight into the impact of human activity pattern changes on air pollution variation. Sci. Total Environ. 732. https://doi.org/10.1016/j.scitotenv.2020.139282.

Lin, C.Y., Wang, Z., Chen, W.N., Chang, S.Y., Chou, C.C.K., Sugimoto, N., Zhao, X., 2007. Long-range transport of Asian dust and air pollutants to Taiwan: observed evidence and model simulation. Atmos. Chem. Phys. 7 (2), 423–434. https://doi.org/10.5194/acp-7-423-2007.

Lin, C.Y., Chou, C.C.K., Wang, Z., Lung, S.C., Lee, C. Te, Yuan, C.S., Chen, W.N., Chang, S.Y., Hsu, S.C., Chen, W.C., Liu, S.C., 2012. Impact of different transport mechanisms of Asian dust and anthropogenic pollutants to Taiwan. Atmos. Environ. 60, 403–418. https://doi.org/10.1016/j.atmosenv.2012.06.049.

Lin, W.Y., Hsiao, M.C., Wu, P.C., Fu, J.S., Lai, L.W., Lai, H.C., 2020. Analysis of air quality and health co-benefits regarding electric vehicle promotion coupled with power plant emissions. J. Clean. Prod. 247, 119152. https://doi.org/10.1016/j.jclepro.2019.119152.

Luo, M., Hou, X., Gu, Y., Lau, N.C., Yim, S.H.L., 2018. Trans-boundary air pollution in a city under various atmospheric conditions. Sci. Total Environ. 618, 132–141. https://doi.org/10.1016/j.scitotenv.2017.11.001.

Matsuda, K., Fujimura, Y., Hayashi, K., Takahashi, A., Nakaya, K., 2010. Deposition velocity of PM2.5 sulfate in the summer above a deciduous forest in central Japan. Atmos. Environ. 44 (36), 4582–4587. https://doi.org/10.1016/j.atmosenv.2010.08.015.

Nguyen, L.S.P., Sheu, G.R., 2019. Four-year measurements of wet mercury deposition at a tropical mountain site in central Taiwan. Aerosol Air Qual. Res. 19 (9), 2043–2055. https://doi.org/10.4209/aaqr.2019.05.0250.

Pani, S.K., Lee, C. Te, Chou, C.C.K., Shimada, K., Hatakeyama, S., Takami, A., Wang, S.H., Lin, N.H., 2017. Chemical characterization of wintertime aerosols over islands and mountains in East Asia: impacts of the continental Asian outflow. Aerosol Air Qual. Res. 17 (12), 3006–3036. https://doi.org/10.4209/aaqr.2017.03.0097.

Querol, X., Alastuey, A., Ruiz, C.R., Artiñano, B., Hansson, H.C., Harrison, R.M., Buringh, E., Ten Brink, H.M., Lutz, M., Bruckmann, P., Straehl, P., Schneider, J., 2004. Speciation and origin of PM10 and PM2.5 in selected European cities. Atmos. Environ. 38 (38), 6547–6555. https://doi.org/10.1016/j.atmosenv.2004.08.037.

Shairsingh, K.K., Jeong, C.H., Evans, G.J., 2019. Transboundary and traffic influences on air pollution across two Caribbean islands. Sci. Total Environ. 653, 1105–1110. https://doi.org/10.1016/j.scitotenv.2018.11.034.

Shimada, K., Yang, X., Araki, Y., Yoshino, A., Takami, A., Chen, X., Meng, F., Hatakeyama, S., 2018. Concentrations of metallic elements in long-range-transported aerosols measured simultaneously at three coastal sites in China and Japan. J. Atmos. Chem. 75 (2), 123–139. https://doi.org/10.1007/s10874-017-9366-8.

Suryani, C.S., Lee, W.J., Endah Mutiara, M.P., Mwangi, J.K., Wang, L.C., Lin, N.H., Chang-Chien, G.P., 2015. Atmospheric deposition of polychlorinated dibenzo-p-dioxins and dibenzofurans at coastal and high mountain areas in Taiwan. Aerosol Air Qual. Res. 15 (4), 1390–1411. https://doi.org/10.4209/aaqr.2015.04.0246.

Tan, P.H., Chou, C., Chou, C.C.K., 2013. Impact of urbanization on the air pollution "holiday effect" in Taiwan. Atmos. Environ. 70, 361–375. https://doi.org/10.1016/j.atmosenv.2013.01.008.

Tseng, Y.L., Yuan, C.S., Bagtasa, G., Chuang, H.L., Li, T.C., 2019. Inter-correlation of chemical compositions, transport routes, and source apportionment results of atmospheric PM2.5 in Southern Taiwan and the Northern Philippines. Aerosol Air Qual. Res. 19 (12), 2645–2661. https://doi.org/10.4209/aaqr.2019.10.0526.

Tumasonis, C.F., Bush, B., Baker, F.D., 1973. PCB levels in egg yolks associated with embryonic mortality and deformity of hatched chicks. Arch. Environ. Contam. Toxicol. 1 (4), 312–324. https://doi.org/10.1007/BF01985433.

Ueda, S., Nakayama, T., Taketani, F., Adachi, K., Matsuki, A., Iwamoto, Y., Sadanaga, Y., Matsumi, Y., 2016. Light absorption and morphological properties of soot-containing aerosols observed at an East Asian outflow site, Noto Peninsula, Japan. Atmos. Chem. Phys. 16 (4), 2525–2541. https://doi.org/10.5194/acp-16-2525-2016.

Vukovich, J., Pierce, T., 2002. The implementation of BEIS3 within the SMOKE modeling framework. Proceedings of the 510 11th International Emissions Inventory Conference, Atlanta, Georgia, April 15–18, 2002.

Wai, K.M., Lin, N.H., Wang, S.H., Dokiya, Y., 2008. Rainwater chemistry at a high-altitude station, Mt. Lulin, Taiwan: comparison with a background station, Mt. Fuji. J. Geophys. Res. Atmos. 113 (6), 1–14. https://doi.org/10.1029/2006JD008248.

Wang, Y., Hao, J., McElroy, M.B., Munger, J.W., Ma, H., Chen, D., Nielsen, C.P., 2009. Ozone air quality during the 2008 Beijing Olympics: effectiveness of emission restrictions. Atmos. Chem. Phys. 9 (14), 5237–5251. https://doi.org/10.5194/acp-9-5237-2009.

Wang, S.H., Lin, N.H., OuYang, C.F., Wang, J.L., Campbell, J.R., Peng, C.M., Lee, C. Te, Sheu, G.R., Tsay, S.C., 2010. Impact of Asian dust and continental pollutants on cloud chemistry observed in northern Taiwan during the experimental period of ABC/EAREX 2005. J. Geophys. Res. Atmos. 115 (19). https://doi.org/10.1029/2009JD013692.

Wang, S.H., Hung, W.T., Chang, S.C., Yen, M.C., 2016. Transport characteristics of Chinese haze over Northern Taiwan in winter, 2005–2014. Atmos. Environ. 126, 76–86. https://doi.org/10.1016/j.atmosenv.2015.11.043.

Wang, Y., Zhang, Y., Schauer, J.J., de Foy, B., Guo, B., Zhang, Y., 2016. Relative impact of emissions controls and meteorology on air pollution mitigation associated with the Asia-Pacific Economic Cooperation (APEC) conference in Beijing, China. Sci. Total Environ. 571, 1467–1476. https://doi.org/10.1016/j.scitotenv.2016.06.215.

Wang, C., Huang, X.-F., Zhu, Q., Cao, L.-M., Zhang, B., He, L.-Y., 2017. Differentiating local and regional sources of Chinese urban air pollution based on the effect of the Spring Festival. Atmos. Chem. Phys. 17, 9103–9114. https://doi.org/10.5194/acp-17-9103-2017.

Wang, P., Chen, K., Zhu, S., Wang, P., Zhang, H., 2020. Severe air pollution events not avoided by reduced anthropogenic activities during COVID-19 outbreak. Resour. Conserv. Recycl. 158 (March), 104814. https://doi.org/10.1016/j.resconrec.2020.104814.

Witte, J.C., Schoeberl, M.R., Douglass, A.R., Gleason, J.F., Krotkov, N.A., Gille, J.C., Pickering, K.E., Livesey, N., 2009. Satellite observations of changes in air quality during the 2008 Beijing Olympics and Paralympics. Geophys. Res. Lett. 36 (17), 1–6. https://doi.org/10.1029/2009GL039236.

Xu, K., Cui, K., Young, L.-H., Hsieh, Y.-K., Wang, Y.-F., Zhang, J., Wan, S., 2020. Part I: impact of the COVID-19 event on air quality in Wuhan, Jingmen, and Enshi cities, China. Aerosol Air Qual. Res. 2, 915–929. https://doi.org/10.4209/aaqr.2020.04.0150.

Zheng, B., Tong, D., Li, M., Liu, F., Hong, C., Geng, G., Li, H., Li, X., Peng, L., Qi, J., Yan, L., Zhang, Y., Zhao, H., Zheng, Y., He, K., Zhang, Q., 2018. Trends in China's anthropogenic emissions since 2010 as the consequence of clean air actions. Atmos. Chem. Phys. 18 (19), 14095–14111. https://doi.org/10.5194/acp-18-14095-2018.